RsOBP2a, a member of OBF BINDING PROTEIN transcription factors, inhibits two chlorophyll degradation genes in green radish

Jiali Ying [a], Jinbin Hu [b], Everlyne M'mbone Muleke [c], Feng Shen [d], Shuangshuang Wen [a], Youju Ye [a], Yunfei Cai [a], Renjuan Qian [a,*]

[a] *Zhejiang Institute of Subtropical Crops, Zhejiang Academy of Agricultural Sciences, 334 Xueshan Road, Wenzhou 325005, Zhejiang, China*
[b] *Ningbo Weimeng Seed Industry Co., Ltd., Ningbo 315100, Zhejiang, China*
[c] *Department of Agriculture and Land Use Management, Masinde Muliro University of Science and Technology, Kenya*
[d] *Jiangsu Coastal Area Institute of Agricultural Sciences, Yancheng 224002, Jiangsu, China*

ARTICLE INFO

ABSTRACT

The green radish (*Raphanus sativus* L.) contains abundant chlorophyll (Chl). DOF-type transcription factor OBF BINDING PROTEIN (OBP) plays crucial functions in plant growth, development, maturation and responses to various abiotic stresses. However, the metabolism by which OBP transcription factors regulate light-induced Chl metabolism in green radish is not well understood. In this study, six *OBP* genes were identified from the radish genome, distributed unevenly across five chromosomes. Among these genes, *RsOBP2a* showed significantly higher expression in the green flesh compared to the white flesh of green radish. Analysis of promoter elements suggested that *RsOBPs* might be involved in stress responses, particularly in light-related processes. Overexpression of *RsOBP2a* led to increase Chl levels in cotyledons and adventitious roots of radish, while silencing *RsOBP2a* expression through TYMV-induced gene silencing accelerated leaf senescence. Further investigations revealed that RsOBP2a was localized in the nucleus and served as a transcriptional repressor. RsOBP2a was induced by light and directly suppressed the expression of *STAYGREEN* (*SGR*) and *RED CHLOROPHYLL CATABOLITE REDUCTASE* (*RCCR*), thereby delaying senescence in radish. Overall, a novel regulatory model involving RsOBP2a, RsSGR, and RsRCCR was proposed to govern Chl metabolism in response to light, offering insights for the enhancement of green radish germplasm.

1. Introduction

The green radish (*Raphanus sativus* L.) is abundant in chlorophyll (Chl), which is one of the most important sensory attributes in consumer preferences for fruit radish. Varieties like the green-skinned 'Xinlimei' and green-fleshed 'Cuishuai' are esteemed for their rich Chl levels, excellent flavor, ornamental value, and potential health benefits [1]. Chl plays a pivotal role in the photosynthesis, facilitating the conversion of light energy into chemical energy [2–4]. Although Chl metabolism has been extensively studied in plant leaves and fruits, there remains a dearth of research in radish taproots [5].

The green color of radish is primarily determined by the accumulation of Chl content or the inhibition of Chl degradation [6]. A distinctive feature known as 'stay-green' characterizes the ability of green radish taproots to maintain their green hue by delaying the breakdown of the photosynthetic apparatus during their formation [69]. While studies have extensively covered Chl synthesis in the green radish, research on the transcriptional regulation of Chl catabolic genes (CCGs) in green radish remains limited [7]. Chl degradation is governed by multiple CCGs [8]. The STAYGREEN (SGR) was identified as a crucial enzyme initiating Chl breakdown in plants [9]. Expression of the *Chlamydomonas reinhardtii SGR* (*CrSGR*) led to a decrease in the Chl content of *Arabidopsis* [10]. In Perennial Ryegrass (*Lolium perenne* L.), *LpSGR* exhibited a higher expression in dark-induced leaf senescence [11,12]. The expression pattern of *NON-YELLOW COLORING 1* (*LpNYC1*) was directly associated with leaf senescence progression [13]. The *NON-YELLOW COLORING 1* (*NYC1*)-*like* gene (*LpNOL*) was highly expressed in senescent leaves [14]. Knocking down *RED CHLOROPHYLL CATABOLITE REDUCTASE* (*RCCR*) led to a significant increase in Chl and carotenoid content in tobacco [15].

Several transcription factors (TFs) have been mined to influence the expression of CCGs in plants, including NAM, ATAF, and CUC (NAC),

---

* Corresponding author.
  E-mail address: qrj@njfu.edu.cn (R. Qian).

WRKY, and DNA BINDING WITH ONE FINGER (DOF) [16,17]. Recent research has confirmed that *Arabidopsis thaliana* NAC046 (ANAC046) serves as a key regulator of leaf senescence by modulating CCGs and senescence-associated genes (SAGs) [18]. The ANAC072 has been found to positively influence dark- and age-induced leaf senescence by activating the *NON-YELLOWING1* (*NYE1*) gene [19–21]. The NAC-LIKE, ACTIVATED BY AP3/PI (PvNAP) has been reported to transactivate the expression of *PvNOL*, *PvSGR*, and *PHEOPHORBIDE a OXYGENASE* (*PvPAO*) genes [22]. ORE1 (ANAC092) plays a significant function in leaf senescence regulator [23]. Notably, *Brassica rapa* WRKY65 (BrWRKY65) directly activates key genes involved in Chl degradation, including *Brassica rapa NYC1* (*BrNYC1*) and *Brassica rapa SGR1* (*BrSGR1*)) [24]. While BrWRKY6 inhibited the expression of *ent-kaurenoic acid hydroxylase 2* (*BrKAO2*) and *gibberellic acid 20-oxidase 2* (*BrGA20ox2*), it can activate *BrSAG12*, *BrNYC1*, and *BrSGR1* [25]. Additionally, Cysteine-rich receptor-like kinase 5 (CRK5) and WRKY53 act as opposing regulators of Chl synthesis, degradation, and senescence in *Arabidopsis thaliana* [26]. Moreover, DOF TFs also played important roles in responding to environmental factors, particularly light and hormonal signals [27]. For instance, ZmDof1 was the first identified *DOF* gene and played a critical role in light-responsive gene expression [28]. In *Arabidopsis*, Dof2.1 promotes JA-induced leaf senescence [29]. Furthermore, *Oryza sativa* DOF24 (OsDOF24) inhibits leaf senescence by deactivating the JA biosynthesis pathway [17]. In young tea (*Camellia sinensis*) leaves, *Camellia sinensis* DOF3 (CsDOF3) and *Camellia sinensis* MYB308 (CsMYB308) form an antagonistic complex regulating transcription of *Camellia sinensis* CLH1 (*CsCLH1*) and Chl content [30,31].

Radish (*Raphanus sativus* L.) holds significant economic importance as a root vegetable crop worldwide. The green radish is abundant in Chl, is increasingly favored in the market. Understanding the molecular regulatory mechanism underlying the coloration of green radish is essential for developing new green radish varieties and ensuring the production of high-quality. Although the involvement of DOF in Chl metabolism has been identified in tea [30,31], the role of OBP TFs in mediating light-induced Chl metabolism in green radish remains unclear. In addition, the availability of several genome sequences makes it feasible to concisely identify and characterize OBP TFs in radish [32]. This study investigated the phylogenetic relationships and expression patterns of OBP family members. Based on transcriptome data from green and white flesh tissues, the expression profiles of *RsOBPs* were analyzed [7]. Furthermore, the involvement of *RsOBP2a* in the regulatory network of coloration in green radish was examined through both overexpression and knock-down experiments to elucidate its role in Chl metabolism. Yeast one-hybrid (Y1H), electrophoretic mobility shift assay (EMSA), and dual-luciferase assay (DLA) were conducted to explore a model linked to RsOBP2a-mediated Chl metabolism in green radish. These findings demonstrate that the light-induced RsOBP2a TF directly binds to *RsSGR* and *RsRCCR* to inhibit Chl metabolism in green taproot, providing valuable insights for enhancing the sensory quality of green radish through genetic improvements.

2. Materials and methods

2.1. Classification of RsOBP members

The conserved DOF domain (PF02701) was extracted from the Pfam database. The four AtOBPs protein sequences were retrieved from the TAIR database and utilized to analyze of the RsOBPs' peptide sequences in radish genome via the BLASTP program [32]. Subsequently, the InterProScan, CDD, and SMART databases were selected to validate the integrity of the DOF domain. The ExPASy ProtParam tool was conducted to analyze the properties of RsOBP proteins.

2.2. Chromosomal location, phylogenetic relationship, and gene structure analysis of RsOBPs

The chromosomal positions of *RsOBPs* were analyzed and displayed by TBtools [33]. To investigate the phylogenetic relationships of RsOBPs, protein sequences from *R. sativus*, *B. rapa*, *Brassica oleracea*, and *A. thaliana* were aligned. Subsequently, the MEGAX software was adopted to construct the phylogenetic tree [34]. The conserved protein motifs and exon-intron structures of RsOBPs were visualized using TBtools. The conserved protein domain of RsOBPs were analyzed with CDD and displayed by TBtools. Furthermore, the conserved protein domains of RsOBP2a and AtOBP2 were aligned using GeneDoc [35].

2.3. cis-regulatory elements (CREs) analysis of RsOBP promoters

The upstream 2 kb promoter sequences of *RsOBP* genes were extracted using TBtools [32,33]. Subsequently, predicted CREs in the upstream promoter regions of *RsOBPs* were identified with PlantCARE, and displayed using TBtools.

2.4. Plant materials and growth conditions

The advanced inbred radish line 'WXQ' with green flesh (GF) aboveground and white flesh (WF) belowground were harvested at 80 d. The GF and WF were rapidly put in liquid nitrogen, and then stored at −80 °C for transcriptome sequencing, respectively. Moreover, *Nicotiana benthamiana* were cultured in a growth chamber with 22 °C 16 h light / 16 °C 8 h dark.

2.5. Analysis the expression levels of RsOBPs

RNA-seq data were extracted from NODAI Radish Genome and employed for the transcriptional profiling of *RsOBP* genes under six different stages (7, 14, 20, 40, 60, and 90 d after sowing) with five different tissues (root tip, leaf, cortex, cambium, and xylem) [36]. The expression patterns of *RsOBPs* under five abiotic stresses (containing heavy metal like cadmium (Cd), chromium (Cr), and lead (Pb), high temperature, and salt stress) were evaluated based on previous RNA-seq studies [37–41]. Furthermore, the expression levels of *RsOBPs* in GF and WF were evaluated using transcriptome data from fruit radish [7]. Heatmaps were generated using TBtools based on $\log_2$-transformed values of fragments per kilobase of transcript per million mapped fragments (FPKM) or Fold Change (FC) information [33].

Total RNA of GF and WF tissues in 'WXQ' were extracted, and the cDNA was synthesized. Real-time quantitative PCR (RT-qPCR) was carried out. The relative expression levels were evaluated with the $2^{-\Delta\Delta CT}$ method. *RsActin* was regarded as the internal reference [42]. Details of the primers used for RT-qPCR are provided in Table S1.

2.6. Promoter activity analysis of RsOBP2a

The 2 kb *RsOBP2a* promoter was integrated into pCAMBIA1391z and pGreenII0800 vectors, respectively. The infiltrated radish cotyledons and tobacco leaves were put in 3 d light or dark conditions, respectively. Subsequently, the GUS staining was adopted to validate the activity of the *RsOBP2a* promoter [43]. Meanwhile, the luminescence (LUC) signals were captured using a Clinx imaging system. Details of the primers used for vector construction are listed in Table S2.

2.7. Vector construction and radish transient transformation

The coding sequence (CDS) of *RsOBP2a* was integrated into pCAMBIA1300-GFP and pTCK303 vectors to produce *35S::RsOBP2a* and *RNAi::RsOBP2a* plasmid, respectively [43]. *A. tumefaciens* strain GV3101 carrying *35S::RsOBP2a*, *RNAi::RsOBP2a*, and the empty vectors (pCAMBIA1300-GFP and pTCK303) were resuspended and employed for

transient transformation of two-week-old radish seedlings. The radish cotyledons infiltrated with the empty vector (EV-OE) and *RsOBP2a*-OE were placed under the dark for 5 d. Correspondingly, the radish cotyledons infiltrated with the empty vector (EV-RNAi) and *RsOBP2a*-RNAi were placed under light for 5 d. The phenotypes of transiently transformed radish cotyledons were assessed, and Chl content and gene expression levels were measured at 5 d post-infiltration [3,4]. The cotyledons under light or dark treatment were used by three independent biological replicates, respectively.

The *35S::RsOBP2a* vector was introduced into *A. rhizogenes* strain MSU440 for genetic transformation in radish [7]. The rootless seedlings of 'LHZ' were used to generate *RsOBP2a-OE* adventitious roots. The transgenic adventitious roots were identified using a LUYOR-3105 UV lamp, and these roots (WT, OE-1, and OE-2) were cultured on MS medium supplemented with 0.3 mg/L NAA and 0.75 mg/L TDZ to induce callus. The Chl content and gene expression levels were also analyzed using three technical repetitions, to investigate the function of *RsOBP2a*.

2.8. Silencing of RsOBP2a in radish

A 40 bp target sequence was selected to construct the pTY-*S* vector for silencing *RsOBP2a* utilizing the *PDS 1000/He* biolistic particle delivery system [44]. The 'YH' seedlings incubated with water were adopted as the negative control. The phenotypes of the silenced plants were observed after 30 d, and the expression patterns of *RsOBP2a* were evaluated.

2.9. Subcellular localization of RsOBP2a

The CDS of *RsOBP2a* without the termination codon was integrated into the pCAMBIA1300-GFP vector. *A. tumefaciens* suspension of empty-GFP vector and recombinant RsOBP2a-GFP vector were infiltrated into tobacco leaves for transient transformation, respectively. Green fluorescence signals were detected using a laser confocal microscope at 48 h post-infiltration (LSM800, Zeiss, Germany).

2.10. Transcription activity analysis of RsOBP2a

To assess the transcriptional activity of RsOBP2a in yeast cells, full length (FL) and truncated fragments (F1, F2, F3, F4, and F5) of RsOBP2a were inserted into pGBKT7 vector to generate the recombinant plasmids. The pGBKT7 and GAL4 served as negative and positive controls, respectively. Each fusion plasmid was transformed into AH109 yeast cells, and then incubated on SD/−Trp and SD/−Trp/-His/−Ade medium at 30 °C for 3 d.

Furthermore, the CDS of *RsOBP2a* was fused into pBD and pBD-VP16 to produce effector. The 5 × GAL4 binding element and a TATA box with the *35S* promoter was ligated into the pGreenII0800 vector to generate reporter. The effector and reporter constructs were transformed into *A. tumefaciens* GV3101 and introduced into tobacco leaves. pBD-VP16 and pBD acted as the positive and negative controls, respectively.

2.11. Yeast one-hybrid (Y1H) assay

The CDS of *RsOBP2a* was inserted into pJG4-5 vector as a prey. The promoter of *RsSGR* and *RsRCCR* (2 kb upstream) and three segmented sub-fragments of *RsRCCR* were fused into pLacZi2μ vector as baits. These plasmids were co-transformed into EGY48 yeast cells. Positive clones were transferred on SD/−Trp−Ura medium with X-Gal for screening after incubation at 28 °C for 3 d. Moreover, the 3 × element (CCGCTTTTTCCCCGCTTTTTCCCCGCTTTTTCC) and 3 × mutation element (CCGCGTGCGCCCCGCGTGCGCCCCGCGTGCGCC) were designed to analyze the binding site of RsOBP2a.

2.12. Electrophoretic mobility shift assay (EMSA)

EMSA was conducted by using the EMSA Kit. The CDS of *RsOBP2a* was fused with pET32a plasmid. The RsOBP2a-pET32a protein was induced in transformed *E. coli* by adding isopropylthio-β-galactoside (IPTG) at a concentration of 0.6 mM. Subsequently, the cells were incubated and purified based on the manufacturer's protocols [45]. The biotin-labeled probes, mutant probes, and unlabeled probes are presented in Table S2.

2.13. Dual luciferase assay (DLA)

The CDS of *RsOBP2a* was integrated into pGreenII62SK vector. The promoters of *RsSGR* and *RsRCCR* (2 kb upstream) were integrated into pGreenII0800 vector, respectively. *A. tumefaciens* culture mixture of *RsOBP2a* TF and *RsSGR/RsRCCR* promoter (in a 10:1 ratio) was infiltrated into 30-day-old tobacco leaves [46]. Subsequently, the LUC signal was detected using the Clinx imaging system 3 d post-infiltration. Additionally, the ratio of firefly luciferase to renilla luciferase (LUC/ REN) activity was measured with the DLA Kit (Vazyme, Nanjing, China).

2.14. Statistical analysis

SPSS 21.0 software (IBM, New York, NY, USA) was adopted for statistical analysis. Variance was performed by the one-way ANOVA and means separated by the Duncan's test. Each error bar represented the standard deviation (SD) from a minimum of three independent replicates. The lowercase letters denote significant differences at $P < 0.05$.

3. Results

3.1. Genome-wide identification of the RsOBP genes

The four AtOBP protein sequences with DOF domain (PF02701) were used as queries. Subsequently, a total of six RsOBPs were identified from the radish genome database, and designated based on their homologous AtOBPs (Table S3). These RsOBPs encoded 252 to 334 amino acids. The molecular weight of these RsOBPs varied from 27.66 kDa to 36.68 kDa. Moreover, the isoelectric points (pI) ranged from 6.58 to 9.56 (Table S3). To analyze the distribution of *RsOBPs* on chromosomes, all *RsOBP* genes were mapped onto the radish genome. These *RsOBPs* are unevenly distributed on five chromosomes, where R1, R5, R8, and R9 each contained one *RsOBP* gene, and R4 contained two *RsOBP* genes (Fig. 1A). Phylogenetic analysis indicated that the six RsOBPs, six BraOBPs, and ten BoOBPs were classified to the same cluster with AtOBPs, suggesting that the OBPs were conserved in Brassicaceae (Fig. 1B, Fig. S1).

To identify the structures of *RsOBP* genes in radish, the exon-intron compositions of the six *RsOBPs* were investigated. Notably, half of the *RsOBPs* (*RsOBP2a*, *RsOBP2b*, and *RsOBP4a*) contained one intron and two exons, and another three *RsOBPs* (*RsOBP3a*, *RsOBP3b*, and *RsOBP4b*) lacked intron, suggesting that these genes along the same branch were similar in gene structures (Fig. 1C). The conserved protein motifs of RsOBPs were characterized by the MEME tool. As a result, both motif 1 and motif 12 were presented in all six RsOBPs (Fig. 1C, Fig. S2). Motif 2 was distributed on four RsOBPs except RsOBP4a and RsOBP4b. Motif 3 was also distributed on four RsOBPs except RsOBP2a and RsOBP2b. Motif 9 was only observed in RsOBP4a and RsOBP4b. Consequently, most of RsOBPs in the same branch exhibited similar motif distribution, indicating that these proteins might have similar constructs and functions.

Five WGD/segmental duplication events involving *RsOBP* genes were identified using the MCScanX software package (Fig. 1D, Table S4). To explore the collinearity analysis of *OBP* genes, a syntenic map was constructed between *R. sativus* and *A. thaliana* (Fig. 1E, Table S5). These findings revealed that there existed six syntenic orthologous gene pairs
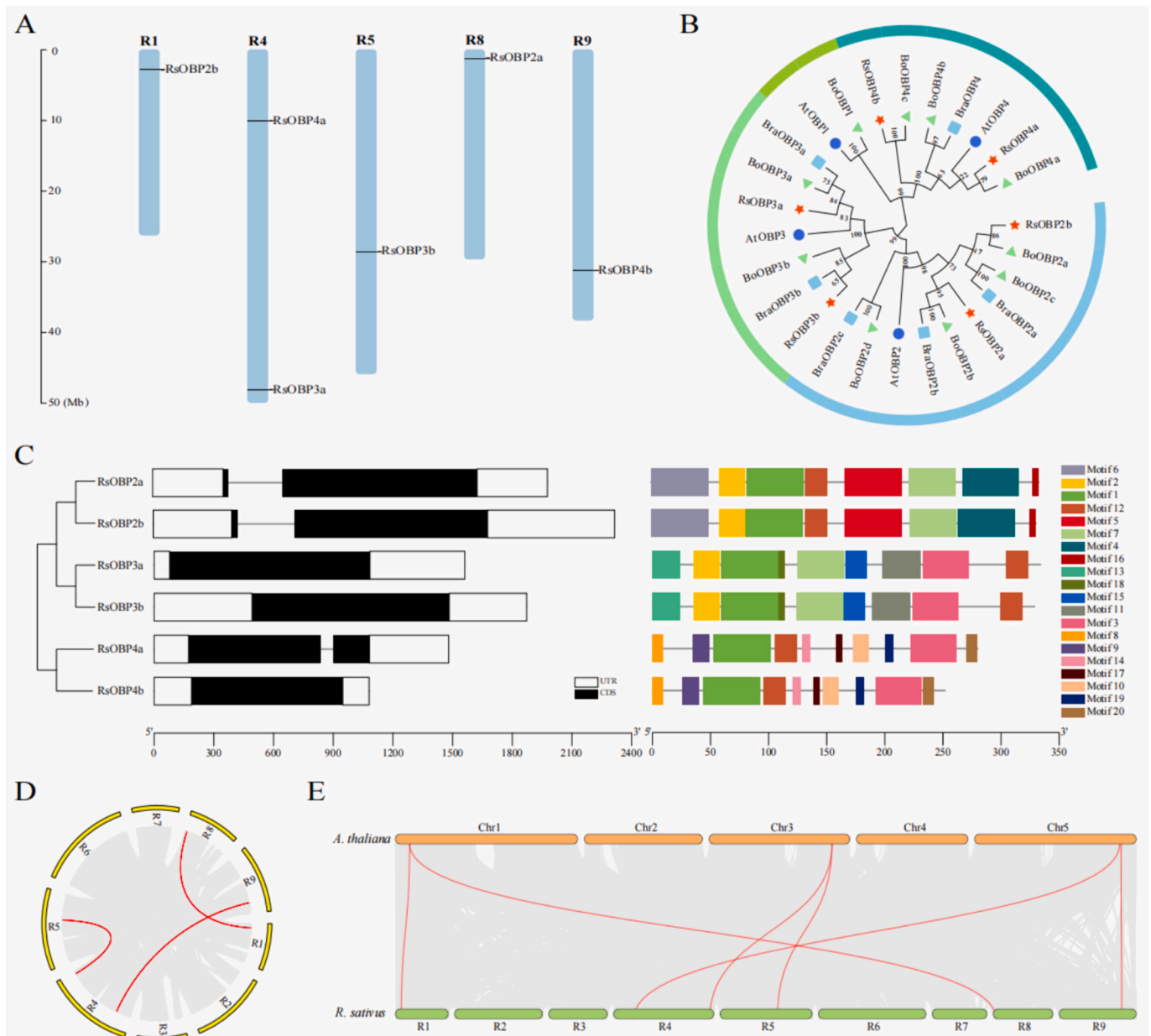
Fig. 1. The identification of six *RsOBPs*. (A) Chromosome distribution of six *RsOBPs*. (B) Phylogenetic tree of RsOBPs. Red stars, royal circles, sky-blue rectangles, and light-green triangles indicated RsOBPs, AtOBPs, BraOBPs, and BoOBPs, respectively. (C) The exon-intron structure and motif distribution of six *RsOBPs*. (D) Distribution and synteny of *RsOBPs*. (E) The collinearity of *OBP* genes between *R. satius* and *A. thaliana*. The red lines indicated *OBP* gene pairs.

between six *RsOBPs* and three *AtOBPs*. These syntenic orthologous genes (one-on-one) were characterized, containing *RsOBP2b-AtOBP2*, *RsOBP4a-AtOBP4*, *RsOBP3a-AtOBP3*, *RsOBP3b-AtOBP3*, *RsOBP2a-AtOBP2*, and *RsOBP4b-AtOBP4*. These gene pairs might have been derived from a common ancestor. Several collinear events indicate that *OBP* genes emerged prior to the lineage divergence between *Arabidopsis* and radish. Furthermore, the Ka/Ks ratio for the three gene pairs was measured, revealing that all *RsOBP* duplication genes exhibited a Ka/Ks < 1, signifying strong purifying selective pressure (Table S6).

3.2. Distribution of CREs in the putative promoter of RsOBP genes

To elucidate the roles of *RsOBPs*, the CREs of 2 kb promoters were analyzed using the PlantCARE database. The CREs of *RsOBP* promoters were involved in 25 functional categories, and classified into four major components, containing development-related, light responsive, hormone responsive, and stress responsive (Fig. 2). Several vital elements (e.g., CAT-box, circadian element, O2-site, and RY-element) were related to plant growth and development, which were located in the promoter of a proportion of *RsOBPs* (Fig. 2A-B). Numerous CREs were participated in several essential phytohormones responses, containing auxin, abscisic acid, methyl jasmonate, and gibberellin responsive elements. The element involved in anaerobic induction (ARE), GC-motif, MYB binding site (MBS), and wound-responsive element (WUN-motif) were presented in the promoter of *RsOBPs*, suggesting that *RsOBPs* might be participated in various stress responses. Notably, each *RsOBP* gene contained at least one light-responsive element (LREs, e.g., ACGT element (ACE), ATCT-motif, G-box, Box 4, GTl-motif, I-box, TCCC-motif, and GATA-motif), indicating that all of these *RsOBPs* might be participated in light response in radish.
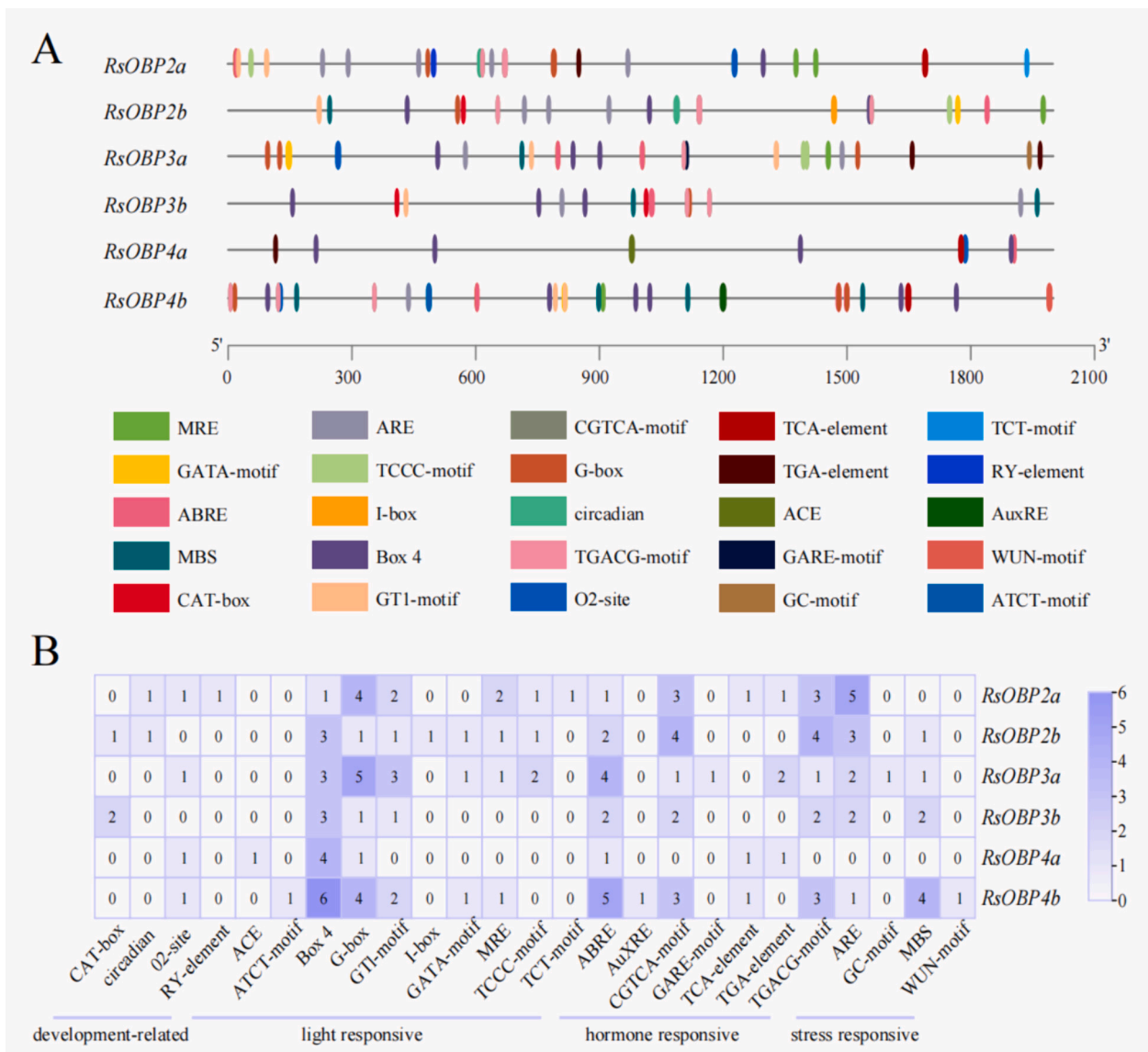
Fig. 2. The characterization of CREs in *RsOBP* promoters. (A) The distribution of CREs in *RsOBP* promoters. (B) The CREs number of *RsOBPs* with different categories.

3.3. The expression patterns of RsOBP genes

The expression profiles of the six *RsOBPs* at different stages with five tissues were estimated using the FPKM method (Fig. S3 A). The findings revealed that a range of *RsOBPs* excepted *RsOBP4b* exhibited high expression levels in root tissue. Particularly, *RsOBP4b* was highly expressed in the 60 d and 90 d cortex. In addition, *RsOBP4a* had high expression levels in all five tissues at every development stage (Fig. S3 A). The differential tissue expression profiles suggested that these *RsOBPs* might play critical roles in several specific tissues in radish, especially in the root. To investigate the potential functions of *RsOBPs* under abiotic stresses, the expression patterns of *RsOBPs* under heavy metal like Cd, Cr, and Pb, heat, and salt stress were analyzed (Fig. S3B). The results revealed that *RsOBP2a*, *RsOBP2b*, *RsOBP3b*, and *RsOBP4a* exhibited significant differences in expression under all abiotic stresses. Moreover, RsOBP3a exhibited high expression levels under Pb, heat, and salt stresses, and *RsOBP4b* demonstrated increased expression levels under heat, Cd, and salt stresses. Overall, these findings suggest a pivotal role for *RsOBP* genes in the growth and development processes of the root.

3.4. RsOBP2a was a light-induced OBP member

According to the transcriptome database, the relative expression patterns of *RsOBP2a* in GF were higher than WF tissue (Fig. 3A). The sequence alignment between RsOBP2a and AtOBP2 indicated that RsOBP2a contained a conserved zinc finger Dof (zf-Dof) domain (Fig. 3B-C). The expression levels of *RsOBPs* further showed that *RsOBP2a* in GF tissue was higher than WF tissue in 'WXQ' (Fig. 3D). Subsequently, pro*RsOBP2a*-GUS was transiently transformed in radish cotyledons and tobacco leaves, and the result showed that GUS activity was enhanced under the 3 d continuous light exposure (Fig. 3E; Fig. 3H). Meanwhile, the LUC signal was significantly increased both in radish cotyledons and tobacco leaves under 3 d continuous light treatment (Fig. 3F-G; Fig. 3I-J). The results collectively revealed that *RsOBP2a* was affected by light and had higher expression levels in the GF than WF tissue of 'WXQ'.

3.5. RsOBP2a increased Chl content in radish cotyledons

In investigating the impact of *RsOBP2a* on Chl metabolism in radish, overexpression and RNA-interference vectors of *RsOBP2a* were adopted
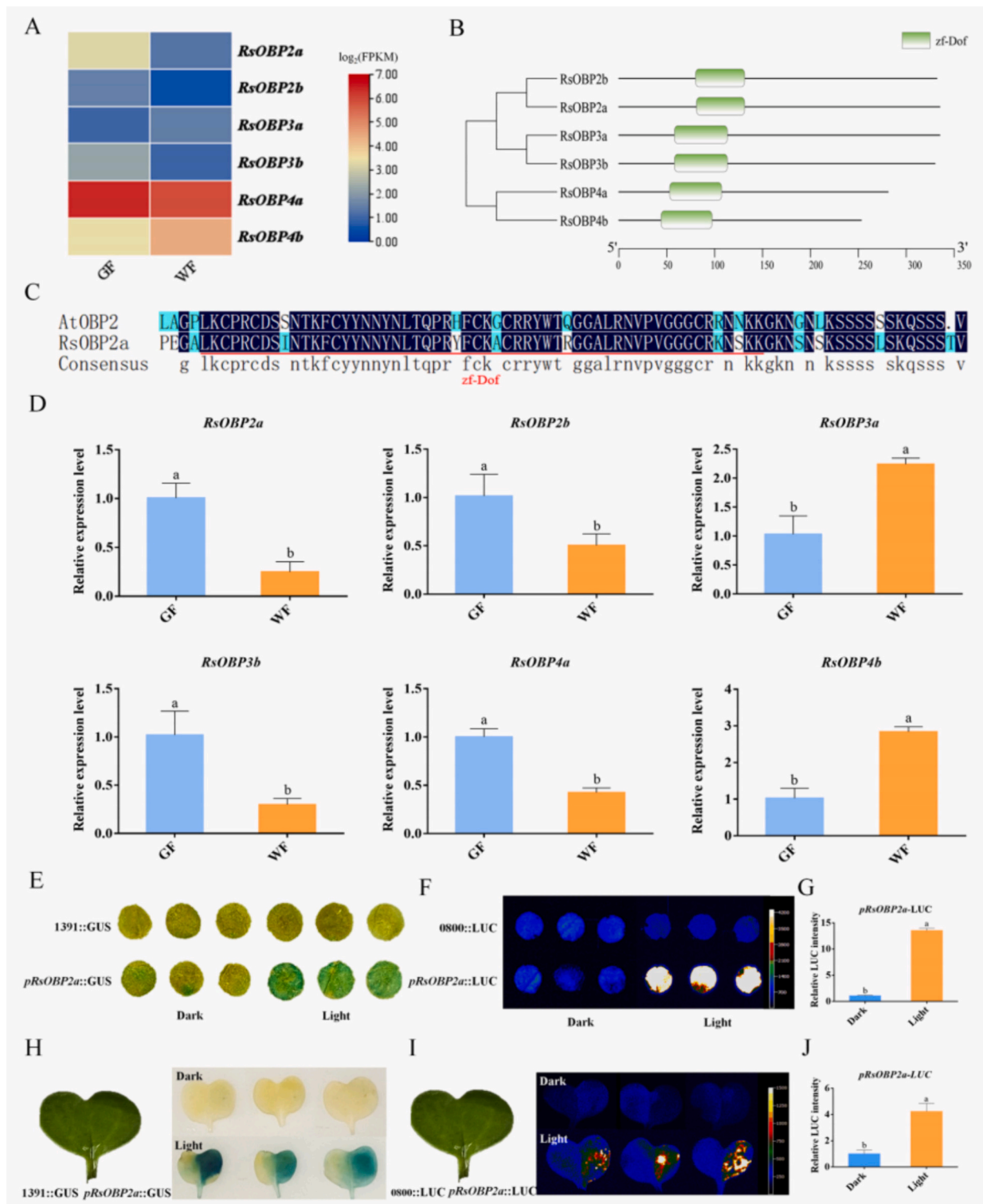
Fig. 3. RsOBP2a is a light-induced member of the RsDOF subgroup. (A). The heatmap of *RsOBPs* in GF and WF tissues based on the previously published transcriptome data. (B). Phylogenetic relationship and architecture of the conserved zf-Dof domain in RsOBPs. (C). Sequence alignment between RsOBP2a and AtOBP2. (D). The expression levels of *RsOBPs* in GF and WF tissues of 'WXQ'. (E). The *RsOBP2a* promoter activity analysis with the GUS report identified tobacco leaves under 3 d continuous light or dark treatment. The 1391 represented the pCAMBIA1391z vector. (F). The *RsOBP2a* promoter activity analysis with LUC reporter assay in tobacco leaves under 3 d continuous light or dark treatment. The 0800 represented the pGreenII0800 vector. (G). Relative LUC intensity of *RsOBP2a* promoter in tobacco leaves under dark and light conditions, respectively. (H). The *RsOBP2a* promoter activity analysis with the GUS report identification in radish cotyledons under 3 d continuous light or dark treatment. The 1391 represented the pCAMBIA1391z vector. (I). The *RsOBP2a* promoter activity analysis with LUC reporter assay in radish cotyledons under 3 d continuous light or dark treatment. The 0800 represented the pGreenII0800 vector. (J). Relative LUC intensity of *RsOBP2a* promoter in radish cotyledons under dark and light conditions, respectively.

for transient transformation in radish cotyledons, respectively. Compared with the control, the color of the radish cotyledons at the injection sites in *RsOBP2a*-OE were darker green (Fig. 4A). In the *RsOBP2a*-OE cotyledons, the content of Chl retained 59.22 %–71.45 % more than EV-OE under five days after dark treatment (5 DAD) (Fig. 4B). The relative expression levels of *RsOBP2a* in *RsOBP2a*-OE cotyledons were significantly higher than those in EV-OE (Fig. 4C).

In contrast, *RsOBP2a*-RNAi cotyledons manifested premature senescence under five days after light treatment (5 DAL). Compared with the control, the injection sites in *RsOBP2a*-RNAi cotyledons displayed lighter green colors (Fig. 4D). The *RsOBP2a*-RNAi cotyledons showed earlier leaf yellowing at 5 DAL, and notably reduced Chl content (Fig. 4D-E). Consistently, the relative expression levels of *RsOBP2a* in *RsOBP2a*-RNAi cotyledons were also lower than those in EV-RNAi at 5 DAL (Fig. 4F). Taken together, these findings suggest that *RsOBP2a* acted as a modulator of Chl metabolism, exerting an inhibitory effect on senescence in radish cotyledons.

3.6. Silencing of RsOBP2a reduced the Chl content

To further elucidate the function of *RsOBP2a*, TYMV-mediated gene silencing technology was employed to knock-down *RsOBP2a*. Compared with the plants inoculated with water, the *RsOBP2a*-silenced plants exhibited prominent chlorosis (Fig. 5A). The Chl content in *RsOBP2a*-silenced plants notably decreased (Fig. 5B). Compared with the control, silencing of *RsOBP2a* resulted in a decrease in the expression levels of *RsOBP2a* in radish leaves (Fig. 5C). These results suggest that *RsOBP2a* might play a potential pivotal function in Chl metabolism within radish leaves.

3.7. Overexpression of RsOBP2a increased the Chl content

To further investigate the effect of *RsOBP2a*, transgenic adventitious roots were identified, among which the overexpression adventitious roots (OE-1 and OE-2) were selected for further functional analysis (Fig. 6A-B). These transgenic adventitious roots were cultured on MS medium supplemented with 0.3 mg/L NAA and 0.75 mg/L TDZ. The Chl
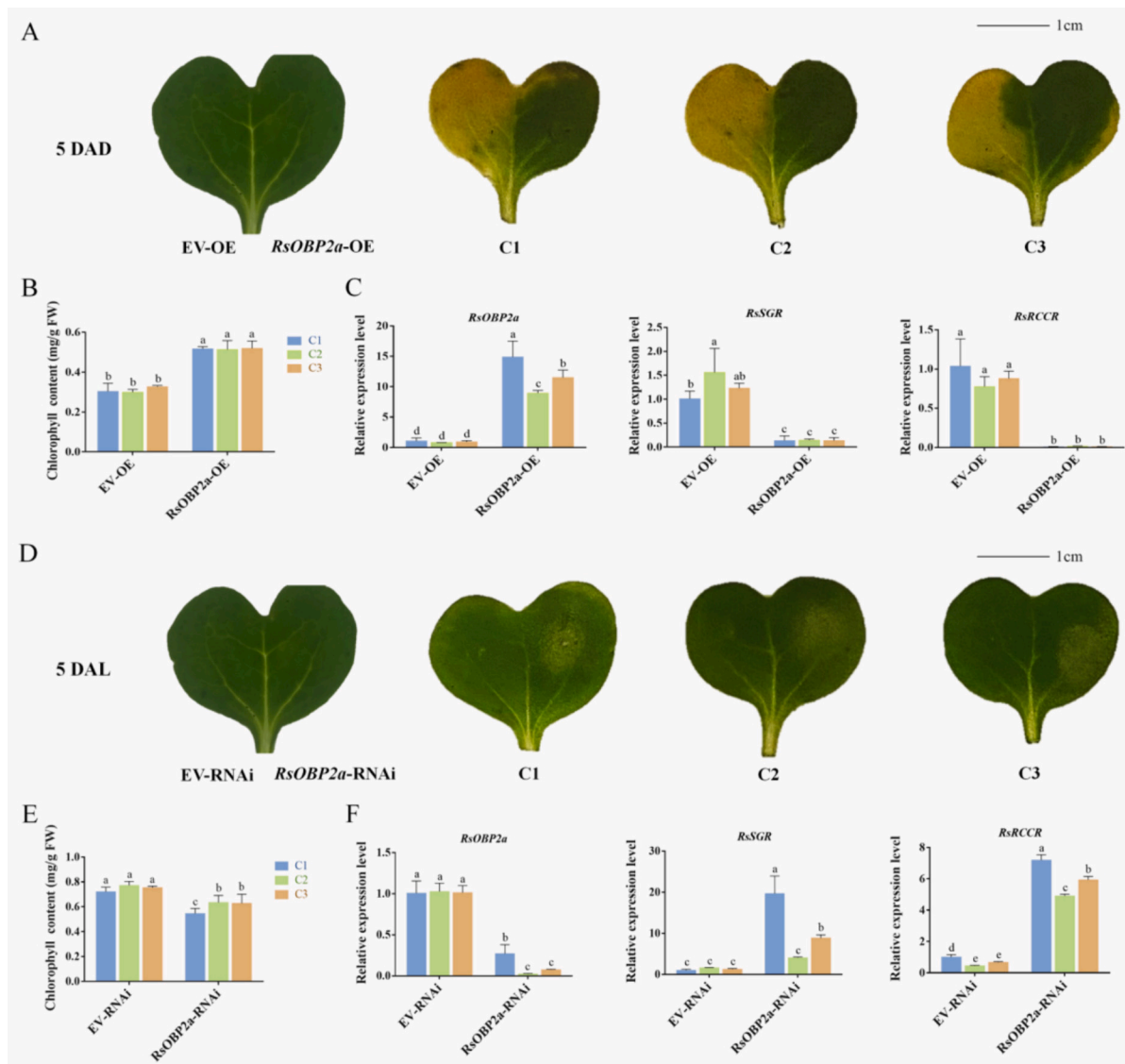
Fig. 4. Functional analysis of *RsOBP2a* in radish cotyledons. (A). The phenotypes of *RsOBP2a*-OE cotyledons under five days after dark treatment (5 DAD). (B). Determination of Chl content in radish cotyledons after 5 DAD. (C). The expression levels of *RsOBP2a*, *RsSGR*, and *RsRCCR* in *RsOBP2a*-OE radish cotyledons after 5 DAD. (D). The phenotypes of *RsOBP2a*-RNAi cotyledons under five days after light treatment (5 DAL). (E). Determination of Chl content of *RsOBP2a*-RNAi cotyledons after 5 DAL. (F). The expression levels of *RsOBP2a*, *RsSGR*, and *RsRCCR* in *RsOBP2a*-RNAi radish cotyledons after 5 DAL.
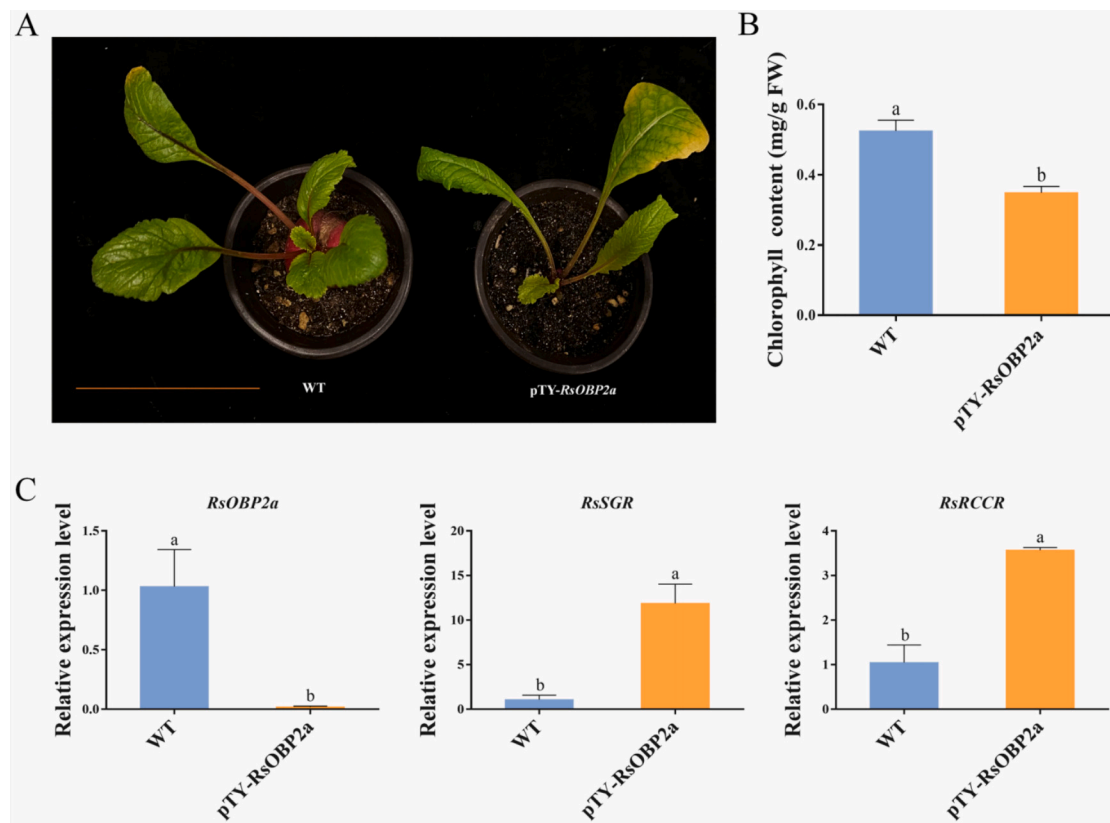
Fig. 5. Silencing of *RsOBP2a* in 'YH' leaves. (A). The phenotypes of *RsOBP2a*-silenced radish. Scale bar: 10 cm. (B). The Chl content determination in *RsOBP2a*-silenced radish leaves. (C). The relative expression levels of *RsOBP2a*, *RsSGR*, and *RsRCCR* in *RsOBP2a*-silenced radish leaves.
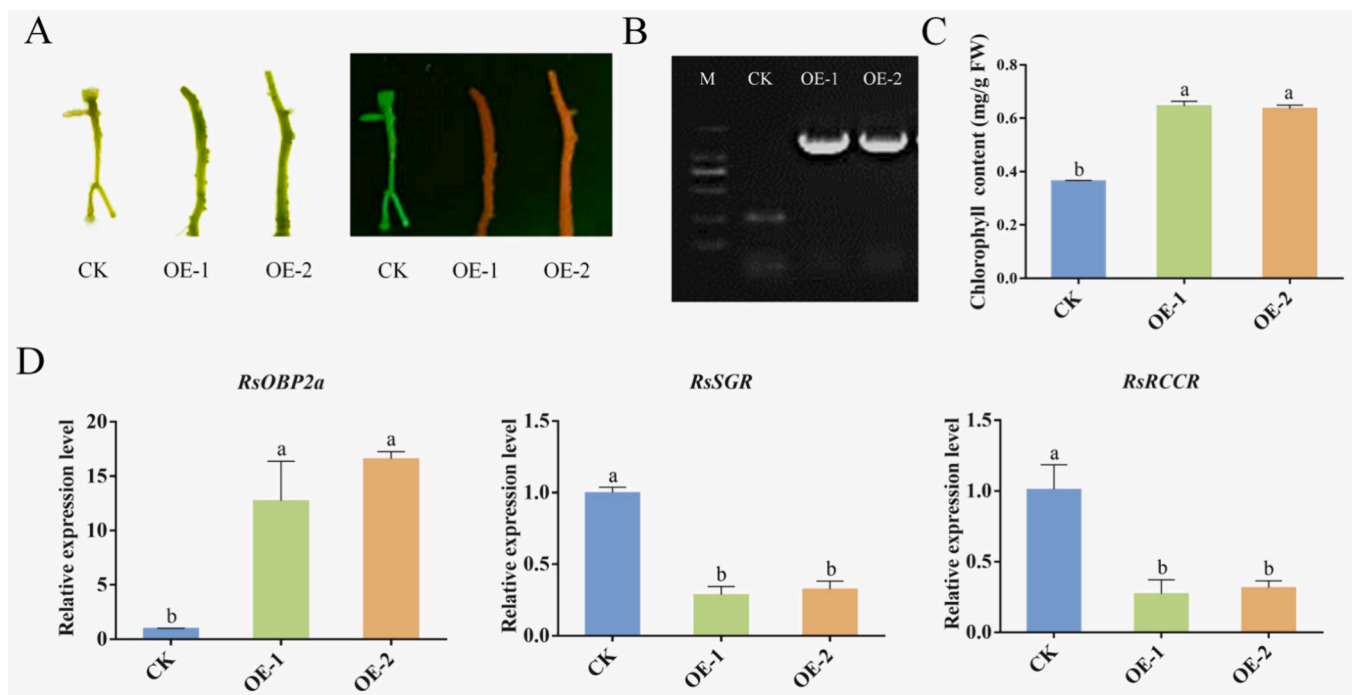
Fig. 6. Overexpression of *RsOBP2a* in radish. (A). The phenotypes of *RsOBP2a*-OE and the control. (B). Electrophoresis identification of *RsOBP2a*-OE adventitious roots. (C). Chl content in *RsOBP2a*-OE adventitious roots. (D). The relative expression levels of *RsOBP2a*, *RsSGR*, and *RsRCCR* in *RsOBP2a*-OE transgenic adventitious roots.

content and relative expression levels of *RsOBP2a* were higher than the control (Fig. 6C-D). These findings indicated that overexpression of *RsOBP2a* increased the Chl content in radish.

3.8. RsOBP2a was a nuclear-localized protein and had transcription inhibitor activity

RsOBP2a-GFP fusion protein and the empty vector were transiently transformed in tobacco leaves. The green fluorescence signal was detected only in the nucleus of RsOBP2a-GFP, suggesting that RsOBP2a was a nuclear protein (Fig. 7A). To evaluate the transcriptional activity of RsOBP2a, the transformants of the full length and truncated RsOBP2a proteins propagated inhibited on SD−Trp/−His/−Ade (Fig. 7B-C). Comparing the β-galactosidase enzyme activities of RsOBP2a and its truncated fragments to pGBKT7 and GAL4, it was evident that RsOBP2a lacked transactivation ability in yeast cells (Fig. 7D). To further assess the transcriptional activity of RsOBP2a in tobacco leaves, the reporter vectors and effector vectors were transiently co-expressed. The result showed that RsOBP2a significantly decreased the expression of the LUC

reporter and VP16 activator in comparison to the effect of pBD and pBD-VP16 vector after 3 d (Fig. 7E-F). These findings demonstrated that RsOBP2a exhibited inhibition ability in yeast cells and tobacco leaves.

3.9. RsOBP2a directly bound to the promoters of RsSGR and RsRCCR and inhibited their expression

To explore whether RsOBP2a directly influences the expression of Chl degradation-related genes in radish, the Y1H assay was conducted. The Y1H results indicated that RsOBP2a could bind to the promoters of *RsSGR* and *RsRCCR* (Fig. 8A). Further Y1H assay using the three truncated promoter fragments (P1, P2, and P3) indicated that RsOBP2a strongly bound to the CTTTTT element within the P2 promoter region of *RsRCCR* (Fig. 8A). However, the interaction did not exist when the CTTTTT element mutated to CGCGTG, revealing that RsOBP2a was a direct upstream regulator of the *RsRCCR* gene and specially bound to CTTTTT region (Fig. 8A). Furthermore, EMSA result demonstrated that the recombinant 32a-RsOBP2a protein bound to the tandem CTTTTT element, indicating that RsOBP2a exerted a direct regulatory effect on
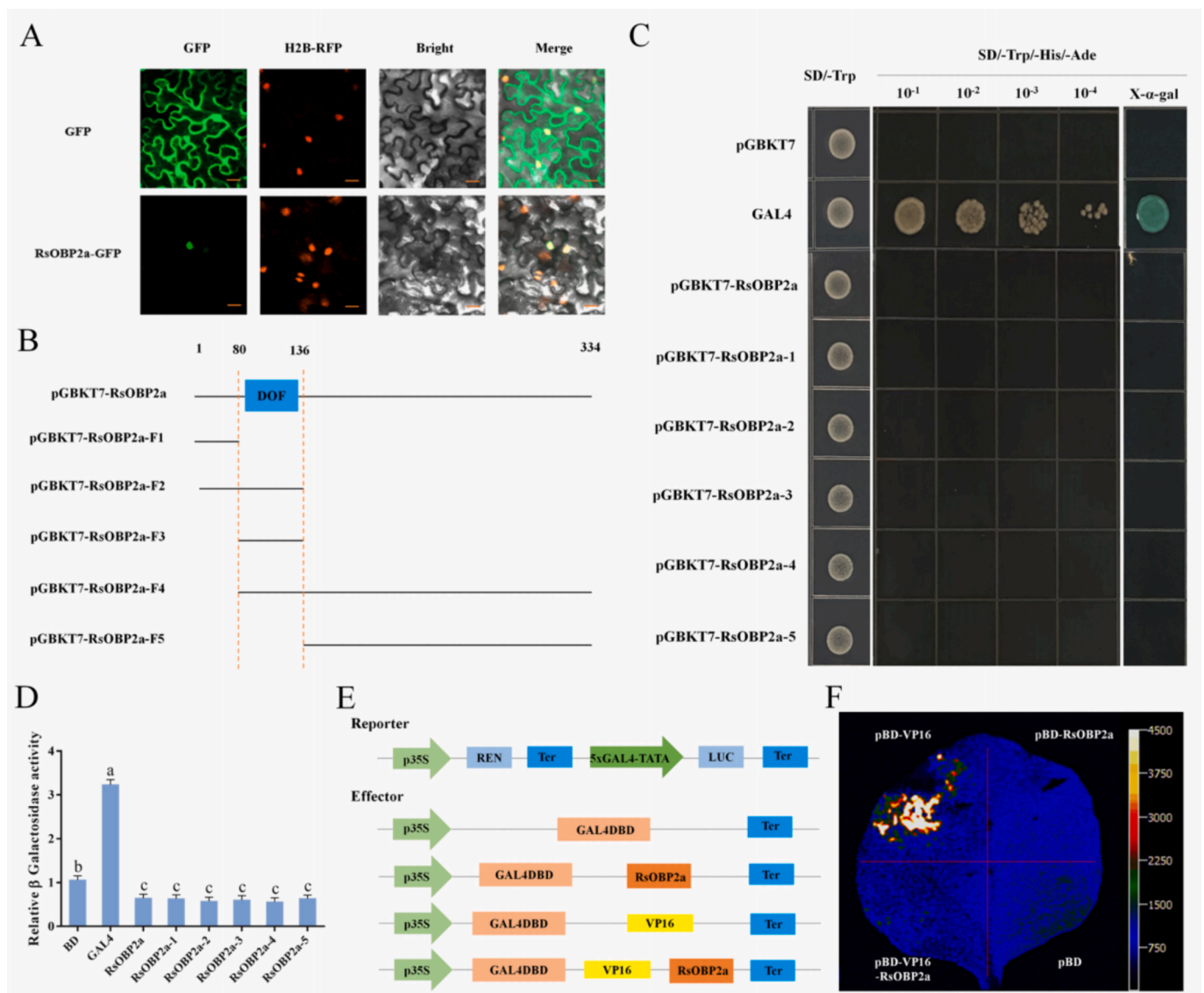
Fig. 7. Subcellular localization and transcriptional activity assay of RsOBP2a. (A). Subcellular localization of RsOBP2a in tobacco leaves. The tobacco were over-expressing an RFP-tag nuclear marker (*35S*::ZmH2B-RFP). (B). Full length and truncated constructs for the RsOBP2a transcriptional activity assay. (C). Transcriptional activity assay of RsOBP2a in the yeast AH109 strain. (D). The detection of β-galactosidase activity. (E). Constructs for LUC reporter assay of RsOBP2a. (F). Observation of LUC signal after 3 d.
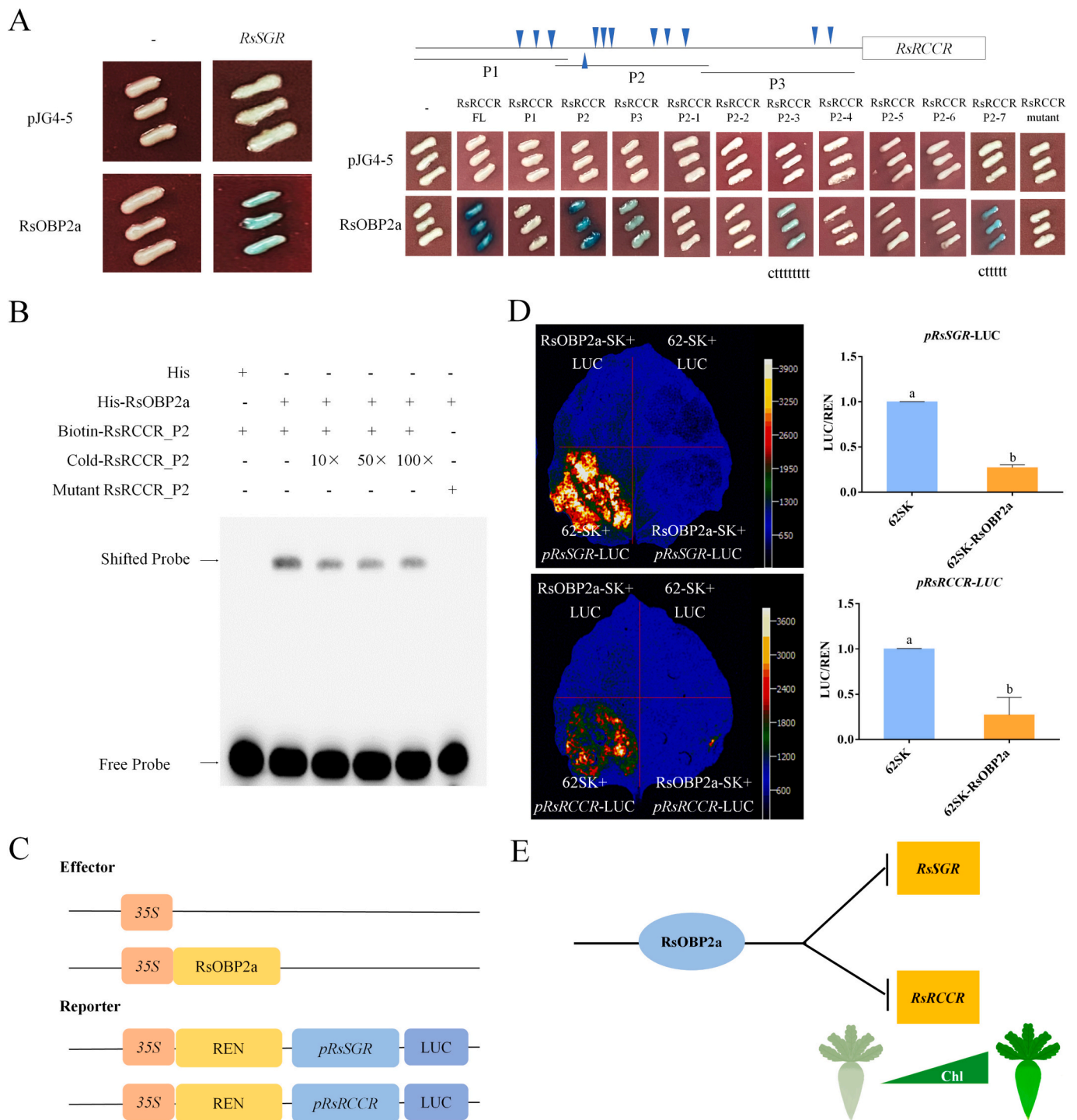
Fig. 8. RsOBP2a inhibited the expression of *RsSGR* and *RsRCCR*. (A). Y1H assay of *RsSGR* and *RsRCCR*. X-Gal was used to analyze the fragment activity. Blue-colored arrowheads indicated the element position of the *RsRCCR* promoter. (B). Analysis of RsOBP2a binding to CTTTTT element using an EMSA system. (C). Constructs used for DLA. (D). Observation of LUC signal in tobacco. Measurement of LUC/REN intensity. The 62SK represented the pGreenII62SK vector. (E). The RsOBP2a-RsSGR/RsRCCR model regulates Chl degradation in the 'WXQ' radish. The green triangle indicates chlorophyll.

RsRCCR (Fig. 8B). DLA showed that RsOBP2a had the ability to inhibit the activity of *RsSGR* and *RsRCCR* promoters (Fig. 8C-D). Moreover, the expression patterns of *RsSGR* and *RsRCCR* were validated by RT-qPCR, and the results indicated that these genes were both significantly down-regulated in *RsOBP2a*-OE radish cotyledons, while up-regulated in *RsOBP2a*-RNAi radish cotyledons (Fig. 4C, Fig. 4F). Moreover, the relative expression levels of *RsSGR* and *RsRCCR* were significantly enhanced in *RsOBP2a*-silenced plants than in the control (Fig. 5C).

Collectively, these findings suggest that RsOBP2a negatively regulates Chl metabolism by inhibiting the expression of *RsSGR* and *RsRCCR* (Fig. 8E).

4. Discussion

Chl plays crucial roles in appeal and quality of green radish. Green flesh is one of the most important agronomic traits that affect the quality

of fruit radish. Previous research demonstrated that the green flesh is distinctive, and the formation of green flesh is attributed to the accumulation of Chl content or the inhibition of Chl degradation [7]. Herein, a light-induced RsOBP2a was identified through transcriptome analysis. The function of *RsOBP2a* was verified by *A. rhizogenes* mediated genetic transformation in radish adventitious roots, as well as through virus-induced gene silencing in radish. Furthermore, the regulatory mechanism of RsOBP2a in Chl metabolism was extensively explored.

4.1. Classification and conserved motifs analysis of RsOBPs

Phylogenetic analysis revealed that the majority of RsOBPs shared closer relationships with BoOBPs and BraOBPs rather than AtOBPs, consistent with the botanical classification within the Brassicaceae family [47]. AtOBP2 displayed 2, 3, and 4 homologous proteins in the genomes of *R. sativus*, *B. rapa*, and *B. oleracea*, respectively, showed that the number of RsOBPs was more than that in *A. thaliana*, but smaller than that of *B. rapa* and *B. oleracea* (Fig. 1B). While gene lengths of RsOBPs varied, MEME analysis revealed a consistent distribution of conserved motifs within *RsOBPs* from the same subgroup (Fig. 1C). Furthermore, RsOBP2a exhibited the lowest instability index and the highest aliphatic index, suggesting that the protein had high stability and thermostability (Table S3).

4.2. RsOBP2a was involved in the light response of radish

DOF TFs are part of the zinc finger protein superfamily, and are specific to plants [48]. DOF TFs generally consist of four critical domains, including oligomerization site, nuclear localization sequence, DOF domains, and transcriptional activation or repression regions [28]. The DOF TFs family has been identified in several horticultural crops, such as tomato, watermelon, Chinese cabbage, and others [48–50]. Among them, OBP TFs play fundamental roles in organ development and tune morphogenesis of plants [51–54]. However, the comprehensive characterization and functional verification of OBP TFs in the coloration of green radish was unexplored. Herein, six RsOBPs were identified by the whole-genome level in radish (Fig. 1A). As shown in Fig. 1C, the exon-intron structure and conserved protein motifs of OBP TFs showed that these proteins were highly conserved evolutionally [55,56]. Furthermore, conserved domain analysis showed that the zf-Dof domain was at the N-terminal of all RsOBP proteins, which were similar to tea, sorghum, and Chinese dwarf cherry [30,31,56]. Notably, multiple CREs related to light responses (e.g., ACE, ATCT-motif, G-box, Box 4, GTl-motif, I-box, TCCC-motif, and GATA-motif) were identified in *RsOBP* promoters, indicating that they might be essential participants in light-mediated biological processes in radish (Fig. 2). Similar CREs were also existed in Chinese dwarf cherry [30,31]. In addition, RT-qPCR analysis revealed that *RsOBPs* showed differential expression patterns in WF and GF tissues of 'WXQ' taproot, indicating that RsOBP TFs might play various roles in regulating the coloration of green radish.

4.3. RsOBP2a negatively regulated Chl metabolism via inhibiting the expression of RsSGR and RsRCCR

The functional characterization of *RsOBP2a* establishes a foundational understanding to elucidate the molecular regulatory network govern by RsOBP in Chl metabolism of green radish. A previous study showed that AtDof1.1 (AtOBP2) acted as a regulator that controlled the biosynthesis of glucosinolate [52]. Overexpression of OBP1 in *Arabidopsis* resulted in significant upregulation of the core cell cycle gene *CYCD3;3* [53]. However, this study showed AtOBP1 had no homology to RsOBP1. The overexpression of AtDOF5.4/OBP4 could promote early occurrence of internal circulation and inhibit cell expansion in *Arabidopsis*, thereby reducing the size and number of transgenic *Arabidopsis* cells, which resulted in dwarfing of transgenic plants [54]. Moreover, the DOF proteins were recognized to target the AAAG/CTTT motif on

promoters [48]. In this study, overexpression of *RsOBP2a* in radish cotyledons and adventitious roots inhibited the expression of *RsSGR* and *RsRCCR*, consequently elevating Chl content (Fig. 4, Fig. 6). On the contrary, transient silencing of *RsOBP2a* enhanced the expression of *RsSGR* and *RsRCCR* while reducing Chl content in radish leaves (Fig. 4, Fig. 5). These findings were consistent with previous studies indicating that DOF was a transcriptional inhibitor involved in light-mediated regulation of Chl anabolism [30,31] (Fig. 7).

The Chl variation phenotype was controlled by complex processes, including induction of CCGs and regulation of TFs [57]. SGR was a senescence-associated gene, which encoded a chloroplast protein [58,59]. In wheat, the expression of *Arabidopsis* LONG HYPOCOTYL IN FAR-RED 1 (AtHFR1) transgene reduced transcript levels of *TaSGR* to delay dark-induced leaf senescence [60]. Overexpression of CsMADS3 TF in citrus calli, tomato, and citrus fruits accelerated Chl degradation and upregulated the *CsSGR* gene [61]. *Litchi chinensis* transcription factor NAC002 (LcNAC002) significantly promotes the expression of *LcSGR* [62]. Therefore, the SGR homologs not only are participated in Chl metabolism during the senescence of green tissues, but also play critical roles in plant development and maturation [63]. Additionally, BALANCE of CHLOROPHYLL METABOLISMs (BCMs) inhibited the Chl degradation in premature and senescent leaves by affecting the activity of SGR [64]. Apart from SGR, other enzymes such as CLH, PAO, PHEOPHYTIN PHEOPHORBIDE HYDROLYASE (PPH), and RCCR are also associated with Chl degradation [65]. In rice, OsPAO and OsRCCR1 contribute significantly to senescence and are involved in wound responses [66]. The overexpression of *Brassica napus gibberellic acid 2-oxidase 6* (*BnGA2ox6*) increased Chl contents, and repressed the expression levels of *CHL1* and *RCCR*, which were related to Chl metabolism [67]. Furthermore, the *Brassica rapa* TEOSINTE BRANCHED1/CYCLOIDEA/PCF (TCP) transcription factor (BrTCP7) positively regulates the expression of the *BrRCCR* [11,12]. *Vitis vinifera* ethylene response factor 17 (VvERF17) was found to regulate Chl degradation by activating genes like *NOL*, *PPH*, *PAO*, and *RCCR* [68]. RsRCCR was the final step in the Chl metabolism pathway, bearing critical importance. In this study, Y1H assays showed that RsOBP2a could bind to *RsSGR* and *RsRCCR in vivo* (Fig. 8A). The EMSA result indicated that RsOBP2a protein interacted with the CTTTTT sequence within the *RsRCCR* promoter (Fig. 8B). Moreover, DLA revealed that RsOBP2a could directly bind to *RsSGR* and *RsRCCR* promoters and significantly repress their activity (Fig. 8C-D). Overall, these findings provide supporting evidences that light responsive factor RsOBP2a acted as an inhibitor in the regulation of Chl metabolism in green radish (Fig. 8E).

5. Conclusion

In summary, *RsOBP2a* was identified from the radish genome, and was found to be a nucleus-localized transcription inhibitor factor. This transcription factor exhibited higher expression in GF tissue of 'WXQ' radish. The transgenic and biochemical analysis revealed that RsOBP2a negatively regulates the expression of Chl metabolism-related genes. Both *in vitro* and *in vivo* experiments demonstrated that RsOBP2a repressed the transcription of *RsSGR* and *RsRCCR* to promote Chl content. Taken together, these findings would facilitate the clarification of the molecular regulatory mechanism underlying RsOBP2a-mediated light response in green radish, and would be beneficial for the cultivation of fruit radish breeding.

CRediT authorship contribution statement

Jiali Ying: Writing – original draft, Validation, Investigation, Formal analysis. **Jinbin Hu:** Writing – original draft, Validation, Investigation, Formal analysis. **Everlyne M'mbone Muleke:** Writing – review & editing. **Feng Shen:** Writing – review & editing. **Shuangshuang Wen:** Writing – original draft, Software. **Youju Ye:** Investigation, Formal analysis. **Yunfei Cai:** Writing – review & editing, Software. **Renjuan**

Qian: Writing – review & editing, Supervision, Methodology, Funding acquisition, Conceptualization.

Declaration of competing interest

The authors declare that they have no known competing financial interests or personal relationships that could have appeared to influence the work reported in this paper.

Data availability

Data will be made available on request.

Acknowledgements

Appendix A. Supplementary data

Supplementary data to this article can be found online at https://doi.org/10.1016/j.ijbiomac.2024.134139.

References

[1] T.J. Liu, Y.J. Zhang, X.H. Zhang, Y.Y. Sun, H.P. Wang, J.P. Song, X.X. Li, Transcriptome analyses reveal key genes involved in skin color changes of 'Xinlimei' radish taproot, Plant Physiol Bioch. 139 (2019) 528–539.

[2] D.I. Arnon, D. Arnon, D. Arnon, Cooper enzymes in isolated chloroplasts polyphenol oxidase in Bet vulgaris, Plant Physiol. 24 (1949) 1–15.

[3] X. Huang, K. Ouyang, Y. Luo, G. Xie, Y. Yang, J. Zhang, A comparative study of characteristics in diploid and tetraploid *Anoectochilus roxburghii*, Front. Nutr. 9 (2022) 1034751.

[4] Y. Huang, L. Cui, W.F. Chen, Z.X. Liu, W.L. Yuan, F.J. Zhu, Z.B. Jiao, Z.X. Zhang, X. H. Deng, L.P. Wang, Z.M. Qiu, C.H. Yan, Comprehensive analysis of NAC transcription factors and their expressions during taproot coloration in radish (*Raphanus sativus* L.), SCI HORTIC-AMSTERDAM. 299 (2022) 111047.

[5] Y.Y. Li, M. Han, R.H. Wang, M.G. Gao, Comparative transcriptome analysis identifies genes associated with chlorophyll levels and reveals photosynthesis in green flesh of radish taproot, PloS One 16 (2021) e0252031.

[6] S.H. Lim, D.H. Kim, J.Y. Lee, RsTTG1, a WD40 protein, interacts with the bHLH transcription factor RsTT8 to regulate anthocyanin and proanthocyanidin biosynthesis in *Raphanus sativus*, Int. J. Mol. Sci. 23 (2022) 11973.

[7] J.L. Ying, Y. Wang, L. Xu, S.Q. Yao, K. Wang, J.H. Dong, Y.B. Ma, L. Wang, Y. Xie, K. Yan, J.X. Li, L.W. Liu, RsGLK2.1-RsNF-YA9a module positively regulates the chlorophyll biosynthesis by activating *RsHEMA2* in green taproot of radish, Plant Sci. 334 (2023) 111768.

[8] G.H. Yu, Z.N. Xie, S.S. Lei, H. Li, B. Xu, B.R. Huang, The NAC factor LpNAL delays leaf senescence by repressing two chlorophyll catabolic genes in perennial ryegrass, Plant Physiol. 189 (2022) 595–610.

[9] D. Dey, D. Dhar, H. Fortunato, D. Obata, A. Tanaka, R. Tanaka, S. Basu, H. Ito, Insights into the structure and function of the rate-limiting enzyme of chlorophyll degradation through analysis of a bacterial Mg-dechelatase homolog, Comput Struct, Biotechnol. J. 19 (2021) 5333–5347.

[10] K. Matsuda, Y. Shimoda, A. Tanaka, H. Ito, Chlorophyll a is a favorable substrate for Chlamydomonas Mg-dechelatase encoded by STAY-GREEN, Plant Physiol Bioch. 109 (2016) 365–373.

[11] B. Xu, G.H. Yu, H. Li, Z.N. Xie, W.W. Wen, J. Zhang, B.R. Huang, Knockdown of *STAYGREEN* in perennial ryegrass (*Lolium perenne* L.) leads to transcriptomic alterations related to suppressed leaf senescence and improved forage quality, Plant Cell Physiol. 60 (2019) 202–212.

[12] Y.M. Xu, X.M. Xiao, Z.X. Zeng, X.L. Tan, Z.L. Liu, J.W. Chen, X.G. Su, J.Y. Chen, BrTCP7 transcription factor is associated with MeJA-promoted leaf senescence by activating the expression of *BrOPR3* and *BrRCCR*, Int. J. Mol. Sci. 20 (2019) 3963.

[13] B. Xu, H. Li, Y. Li, G.H. Yu, J. Zhang, B.R. Huang, Characterization and transcriptional regulation of chlorophyll b reductase gene *NON-YELLOW COLORING 1* associated with leaf senescence in perennial ryegrass (*Lolium perenne* L.), Environ. Exp. Bot. 149 (2018) 43–50.

[14] G.H. Yu, Z.N. Xie, J. Zhang, S.S. Lei, W.J. Lin, B. Xu, B.R. Huang, *NOL*-mediated functional stay-green traits in perennial ryegrass (*Lolium perenne* L.) involving multifaceted molecular factors and metabolic pathways regulating leaf senescence, Plant J. 106 (2021) 1219–1232.

[15] C. Dong, M. Zhang, F. Wei, et al., Inhibition of red chlorophyll catabolite reductase improved chlorophyll and carotenoid synthesis in tobacco, Plant Cell Tissue Organ Cult. 148 (2022) 687–698.

[16] Y. Guo, G. Ren, K. Zhang, Z. Li, Y. Miao, H. Guo, Leaf senescence: progression, regulation, and application, Mol Hortic. 1 (2021) 1–25.

[17] Y. Shim, K. Kang, G. An, N.C. Paek, Rice DNA-binding One Zinc Finger 24 (OsDOF24) delays leaf senescence in a jasmonate-mediated pathway, Plant Cell Physiol. 60 (2019) 2065–2076.

[18] C. Oda-Yamamizo, N. Mitsuda, S. Sakamoto, et al., The NAC transcription factor ANAC046 is a positive regulator of chlorophyll degradation and senescence in *Arabidopsis* leaves, Sci. Rep. 6 (2016) 23609.

[19] H. Li, W. Huang, Z.W. Liu, Y.X. Wang, J. Zhuang, Transcriptome-Based Analysis of Dof Family Transcription Factors and Their Responses to Abiotic Stress in Tea Plant (*Camellia sinensis*), Int J Genomics. 2016 (2016) 5614142.

[20] S. Li, J. Gao, L. Yao, et al., The role of ANAC072 in the regulation of chlorophyll degradation during age- and dark-induced leaf senescence, Plant Cell Rep. 35 (2016) 1729–1741.

[21] Z. Li, Z.L. Ren, F.Q. Tan, Z.X. Tang, S.L. Fu, B.J. Yan, T.H. Ren, Molecular cytogenetic characterization of new Wheat-Rye 1R(1B) substitution and translocation lines from a Chinese *Secale cereal* L, *Aigan* with resistance to stripe rust, PLoS ONE. 11 (2016) e0163642.

[22] Z.N. Xie, G.H. Yu, S.S. Lei, H. Wang, B. Xu, STRONG STAYGREEN inhibits DNA binding of PvNAP transcription factors during leaf senescence in switchgrass, Plant Physiol. 190 (2022) 2045–2058.

[23] I. Chun, H.J. Kim, S. Hong, Y.G. Kim, M.S. Kim, Structural basis of DNA binding by the NAC transcription factor ORE1, a master regulator of plant senescence, Plant Communications. 4 (2023) 100510.

[24] Z.Q. Fan, X.L. Tan, W. Shan, J.F. Kuang, W.J. Lu, J.Y. Chen, BrWRKY65, a WRKY transcription factor, is involved in regulating three leaf senescence-associated genes in Chinese Flowering Cabbage, Int. J. Mol. Sci. 18 (2017) 1228.

[25] Z.Q. Fan, X.L. Tan, W. Shan, J.F. Kuang, et al., Characterization of a transcriptional regulator, BrWRKY6, associated with gibberellin-suppressed leaf senescence of Chinese Flowering Cabbage, J Agr Food Chem. 66 (2018) 1791–1799.

[26] P. Burdiak, J. Mielecki, P. Gawroński, S. Karpiński, The CRK5 and WRKY53 are conditional regulators of senescence and stomatal conductance in *Arabidopsis*, Cells 11 (2022) 3558.

[27] X.Y. Tao, M.L. Li, T. Zhao, S.L. Feng, H.L. Zhang, L.Y. Wang, J. Han, M.T. Gao, K. N. Lu, Q.J. Chen, B.L. Zhou, X.Y. Guan, Neofunctionalization of a polyploidization-activated cotton long intergenic non-coding RNA DAN1 during drought stress regulation, Plant Physiol. 186 (2021) 2152–2168.

[28] S. Yanagisawa, J. Sheen, Involvement of maize Dof zinc finger proteins in tissue-specific and light-regulated gene expression, Plant Cell 10 (1998) 75–89.

[29] M. Zhuo, Y. Sakuraba, S. Yanagisawa, A Jasmonate-activated MYC2-Dof2.1-MYC2 transcriptional loop promotes leaf senescence in *Arabidopsis*, Plant Cell 32 (2020) 242–262.

[30] W.L. Liu, W.C. Ren, X.B. Liu, L.Q. He, C. Qin, P.P. Wang, L.Y. Kong, Y. Li, Y.W. Liu, W. Ma, Identification and characterization of *Dof* genes in *Cerasus humilis*, Front, Plant Sci. 14 (2023) 1–10.

[31] W.M. Liu, S.Y. Liu, K.Y. Zhang, M.W. Xie, H.W. Sun, X.Q. Huang, L.X. Zhang, M. Li, Chlorophyllase is transcriptionally regulated by CsMYB308/CsDOF3 in young leaves of tea plant, Horticultural, Plant J. 9 (2023), 2468–0141.

[32] Y.M. Jeong, N. Kim, B.O. Ahn, M. Oh, W.H. Chun, H. Chun, et al., Elucidating the triplicated ancestral genome structure of radish based on chromosome-level comparison with the Brassica genomes, Theor. Appl. Genet. 129 (2016) 1357–1372.

[33] C.J. Chen, H. Chen, Y. Zhang, H.R. Thomas, M.H. Frank, Y.H. He, R. Xia, TBtools-an integrative toolkit developed for interactive analyses of big biological data, Mol. Plant 13 (2020) 8.

[34] S. Kumar, G. Stecher, M. Li, C. Knyaz, K. Tamura, MEGA X: molecular evolutionary genetics analysis across computing platforms, Mol. Biol. Evol. 35 (2018) 1547–1549.

[35] K.B. Nicholas, H.B. Nicholas, GeneDoc: a tool for editing and annotating multiple sequence alignments, Embnet News. 4 (1997) 1023–4144.

[36] Y. Mitsui, M. Shimomura, K. Komatsu, N. Namiki, M. Shibata-Hatta, M. Imai, Y. Katayose, Y. Mukai, H. Kanamori, K. Kurita, et al., The radish genome and comprehensive gene expression profile of tuberous root formation and development, Sci. Rep. 5 (2015) 10835.

[37] X. Sun, L. Xu, Y. Wang, X. Luo, X. Zhu, K.B. Kinuthia, S. Nie, H. Feng, C. Li, L. Liu, Transcriptome-based gene expression profiling identifies differentially expressed genes critical for salt stress response in radish (*Raphanus sativus* L.), Plant Cell Rep. 35 (2016) 329–346.

[38] R. Wang, Y. Mei, L. Xu, X. Zhu, Y. Wang, J. Guo, L. Liu, Genome-wide characterization of differentially expressed genes provides insights into regulatory network of heat stress response in radish (*Raphanus sativus* L.), Funct. Integr. Genomics 18 (2018) 225–239.

[39] Y. Wang, L. Xu, Y. Chen, H. Shen, Y. Gong, C. Limera, L. Liu, Transcriptome profiling of radish (*Raphanus sativus* L.) root and identification of genes involved in response to Lead (Pb) stress with next generation sequencing, PloS One 8 (2013) e66539.

[40] Y. Xie, S. Ye, Y. Wang, L. Xu, X. Zhu, J. Yang, H. Feng, R. Yu, B. Karanja, Y. Gong, L. Liu, Transcriptome-based gene profiling provides novel insights into the characteristics of radish root response to Cr stress with next-generation sequencing, Front. Plant Sci. 6 (2015) 202.

[41] L. Xu, Y. Wang, W. Liu, J. Wang, X. Zhu, K. Zhang, R. Yu, R. Wang, Y. Xie, W. Zhang, Y. Gong, L. Liu, *De novo* sequencing of root transcriptome reveals

complex cadmium-responsive regulatory networks in radish (*Raphanus sativus* L.), Plant Sci. 236 (2015) 313–323.

[42] K.J. Livak, T.D. Schmittgen, Analysis of relative gene expression data using real-time quantitative PCR and the $2^{-\Delta\Delta CT}$ method, Methods 25 (2002) 402–408.

[43] K. Wang, L. Xu, Y. Wang, J.L. Ying, J.X. Li, J.H. Dong, C. Li, X.L. Zhang, L.W. Liu, Genome-wide characterization of homeodomain-leucine zipper genes reveals *RsHDZ17* enhances the heat tolerance in radish (*Raphanus sativus* L.), Physiol. Plant. 174 (2022) e13789.

[44] Y. Wang, J.L. Ying, Y. Zhang, L. Xu, W.T. Zhang, M. Ni, Y.L. Zhu, L.W. Liu, A genome-wide identification and functional characterization of the Cation Proton Antiporter (CPA) family related to salt stress response in radish (*Raphanus sativus* L.), Int. J. Mol. Sci. 21 (2020) 8262.

[45] S.H. Jiang, M. Chen, N.B. He, X.L. Chen, N. Wang, Q.G. Sun, T.L. Zhang, H.F. Xu, H. C. Fang, Y.C. Wang, MdGSTF6, activated by MdMYB1, plays an essential role in anthocyanin accumulation in apple, Hortic Res. 6 (2019) 40.

[46] L.X. Fan, Y. Wang, L. Xu, M.J. Tang, X.L. Zhang, J.L. Ying, C. Li, J.H. Dong, L. W. Liu, A genome–wide association study uncovers a critical role of the *RsPAP2* gene in red-skinned *Raphanus sativus* L, Hortic Res. 7 (2020) 164.

[47] H. Kobayashi, K. Shirasawa, N. Fukino, H. Hirakawa, T. Akanuma, H. Kitashiba, Identification of genome-wide single-nucleotide polymorphisms among geographically diverse radish accessions, DNA Res. 27 (2020) 1–7.

[48] S. Gupta, N. Malviya, H. Kushwaha, J. Nasim, N.C. Bisht, V.K. Singh, D. Yadav, Insights into structural and functional diversity of Dof (DNA binding with one finger) transcription factor, Planta 241 (2015) 549–562.

[49] J. Ma, M.Y. Li, F. Wang, J. Tang, A.S. Xiong, Genome-wide analysis of Dof family transcription factors and their responses to abiotic stresses in Chinese cabbage, BMC Genomics 16 (2015) 33.

[50] M. Noguero, R.M. Atif, S. Ochatt, R.D. Thompson, The role of the DNA-binding One Zinc Finger (DOF) transcription factor family in plants, Plant Sci. 209 (2013) 32–45.

[51] B. Rymen, A. Kawamura, S. Schäfer, et al., ABA Suppresses Root Hair Growth via the OBP4 Transcriptional Regulator, Plant Physiol. 173 (2017) 1750–1762.

[52] A. Skirycz, M. Reichelt, M. Burow, C. Birkemeyer, J. Rolcik, J. Kopka, M.I. Zanor, J. Gershenzon, M. Strnad, J. Szopa, B. Mueller-Roeber, I. Witt, DOF transcription factor AtDof1.1 (OBP2) is part of a regulatory network controlling glucosinolate biosynthesis in *Arabidopsis*, Plant J. 47 (2006) 10–24.

[53] A. Skirycz, A. Radziejwoski, W. Busch, M.A. Hannah, J. Czeszejko, M. Kwaśniewski, M.I. Zanor, J.U. Lohmann, V.L. De, I. Witt, B. Mueller-Roeber, The DOF transcription factor OBP1 is involved in cell cycle regulation in *Arabidopsis thaliana*, Plant J. 56 (2008) 779–792.

[54] P. Xu, H. Chen, L. Ying, et al., AtDOF5.4/OBP4, a DOF transcription factor gene that negatively regulates cell cycle progression and cell expansion in *Arabidopsis thaliana*, Sci. Rep. 6 (2016) 27705.

[55] A.R. Corrales, S.G. Nebauer, L. Carrillo, et al., Characterization of tomato cycling Dof factors reveals conserved and new functions in the control of flowering time and abiotic stress responses, J. Exp. Bot. 65 (2014) 995–1012.

[56] Q. Xiao, T. Liu, M. Ling, Q. Ma, W. Cao, F. Xing, T. Huang, Y. Zhang, H. Duan, Z. Liu, Genome-Wide Identification of DOF Gene Family and the Mechanism Dissection of SbDof21 Regulating Starch Biosynthesis in Sorghum, Int. J. Mol. Sci. 23 (2022) 12152.

[57] H. Fang, P. Wang, F. Ye, J. Li, M. Zhang, C. Wang, W. Liao, Genome-wide identification and characterization of the Calmodulin-Binding Transcription Activator (CAMTA) gene family in plants and the expression pattern analysis of *CAMTA3/SR1* in tomato under abiotic stress, Int. J. Mol. Sci. 23 (2022) 6264.

[58] L.A.J. Mur, S. Aubry, M. Mondhe, A. Kingston-Smith, J. Gallagher, E. Timms-Taravella, C. James, I. Papp, S. Hörtensteiner, H. Thomas, H. Ougham, Accumulation of chlorophyll catabolites photosensitizes the hypersensitive response elicited by Pseudomonas syringae in *Arabidopsis*, New Phytol. 188 (2010) 161–174.

[59] S.Y. Park, W. Yu, J.S. Park, et al., The senescence-induced staygreen protein regulates chlorophyll degradation, Plant Cell 19 (2007) 1649–1664.

[60] G. Sun, L. Yang, W. Zhan, S. Chen, M. Song, L. Wang, L. Jiang, L. Guo, K. Wang, X. Ye, M. Gou, X. Zheng, J. Yang, Z. Yan, HFR1, a bHLH transcriptional regulator from *Arabidopsis thaliana*, improves grain yield, shade and osmotic stress tolerances in common wheat, Int. J. Mol. Sci. 23 (2022) 12057.

[61] K.J. Zhu, H.Y. Chen, X.H. Mei, et al., Transcription factor CsMADS3 coordinately regulates chlorophyll and carotenoid pools in *Citrus* hesperidium, Plant Physiol. 193 (2023) 519–536.

[62] S.C. Zou, M.G. Zhuo, F. Abbas, G.B. Hu, H.C. Wang, X.M. Huang, Transcription factor LcNAC002 coregulates chlorophyll degradation and anthocyanin biosynthesis in litchi, Plant Physiol. 192 (2023) 1913–1927.

[63] B. Jiao, Q. Meng, W. Lv, Roles of stay-green (SGR) homologs during chlorophyll degradation in green plants, Bot. Stud. 61 (2020) 25.

[64] H. Yamatani, T. Ito, K. Nishimura, T. Yamada, W. Sakamoto, M. Kusaba, Genetic analysis of chlorophyll synthesis and degradation regulated by BALANCE of CHLOROPHYLL METABOLISM, Plant Physiol. 189 (2022) 419–432.

[65] B. Lai, B. Hu, Y.H. Qin, J.T. Zhao, H.C. Wang, G.B. Hu, Transcriptomic analysis of *Litchi chinensis* pericarp during maturation with a focus on chlorophyll degradation and flavonoid biosynthesis, BMC Genomics 16 (2015) 225.

[66] Y.Y. Tang, M.R. Li, Y.P. Chen, et al., Knockdown of *OsPAO* and *OsRCCR1* cause different plant death phenotypes in rice, J. Plant Physiol. 168 (2011) 1952–1959.

[67] J.D. Yan, X.Y. Liao, R.Q. He, et al., Ectopic expression of GA 2-oxidase 6 from rapeseed (*Brassica napus* L.) causes dwarfism, late flowering and enhanced chlorophyll accumulation in *Arabidopsis thaliana*, Plant Physiol Bioch. 111 (2017) 10–19.

[68] S.W. Lu, M.W. Zhang, Y.X. Zhuge, et al., VvERF17 mediates chlorophyll degradation by transcriptional activation of chlorophyll catabolic genes in grape berry skin, Environ. Exp. Bot. 193 (2022) 104678.

[70] Z. Li, Q. Jiang, T. Fan, L.Q. Zhao, Z.L. Ren, F.Q. Tan, P.G. Luo, T.H. Ren, Molecular Cytogenetic and Physiological Characterization of a Novel Wheat-Rye T1RS.1BL Translocation Line from *Secale cereal* L. Weining with Resistance to Stripe Rust and Functional "Stay Green", Trait. Int. J. Mol. Sci. 23 (2022) 4626.